

Probabilistic Range Query over Uncertain Moving Objects in Constrained 2D Space

Zhi Jie Wang Donghua Wang Bin Yao

Department of Computer Science and Engineering,
Shanghai Jiao Tong University, Shanghai 200240, China
{zjwang888, dhwang, binyao}@sjtu.edu.cn

Abstract. Recently, probabilistic range query (PRQ) over uncertain moving objects has attracted more and more attentions, due to the fact it can help people extract their interested moving objects with quantitative probability. Previous works usually assumed objects moving on a well defined route, or assumed objects moving freely in 2D space. The first assumption is appropriate for query processing on road networks (called “qRN” for convenience) where the roads are represented as a series of line segments. This assumption, however, can not work for query processing on region (called “qR”). In contrast, the second assumption is suitable for “qR”, but it is impractical in real applications since various obstacles may limit the movement of moving objects. In this paper, we introduce the concept of restricted areas, and we are interested in “qR”. Specifically, we consider the problem of PRQ over uncertain moving objects in constrained 2D space. To achieve these goals is significant, since it is closer to the real applications, and contributes to returning more authentic answers. In order to tackle the above problem, we proposed our solution and demonstrated the effectiveness and efficiency of our proposed approaches by extensive experiments under various experimental settings.

1 Introduction

Recently, with the rapid development of positioning technologies like GPS, RFID and WSN, as well as the broad application of Location-Based Services [1] in many scenarios such as digital battlefield, traffic control, mobile workforce management, transportation industry and so on, range query as one of common operation in moving object database has been attracting more and more attentions [2–11]. In general, mobile objects report their locations to corresponding server through a wireless interface, or the objects are tracked through ground-based radars or satellites. However, positioning technologies as well as other manners still cannot assure 100% accuracy, namely, the data we acquired itself may be not completely correct comparing to the real physical locations [12]. Moreover, due to limited network bandwidth and limited battery power of the mobile devices, it is often infeasible, for the database, to contain the total status of an entity (which is monitored at every moment in time) [13], so we just can obtain discrete location information, that is, the specific position between

two continuous sampling is uncertain. In order to alleviate these problems, the idea of incorporating uncertainty into moving objects data has been proposed [14]. A common model for characterizing the location uncertainty of an object is a closed region together with a probability density function (*pdf*) [15, 13, 14, 16–19]. Simply speaking, this model assumes the object can be always found in the closed region, and assume the specific location of the object is subjected to certain distribution (e.g., uniform distribution) in this closed region.

In the literature of moving object database, there already was a large bulk of works on PRQ over uncertain moving objects [19, 20, 12, 21, 22, 16, 23, 24, 13, 17]. On the whole, previous works usually assumed objects moving on a well defined route [25, 14], or assumed objects moving freely in 2 dimensional space [16, 19]. The first assumption is suitable for “qRN”. For example, a frequently used method for “qRN” is using a graph to denote road networks, where roads are took as a series of line segments. This assumption, however, can not work for “qR”. In contrast, the second assumption is suitable for “qR”, but it is impractical in realistic applications, since there are various obstacles that limit the movement of objects. For example, an automobile usually cannot run in a lake or river. In this paper, we introduce the concept of restricted area, and we are interested in “qR”. Obviously, that we introduce some restricted areas is meaningful. First, it is more coming close to the real applications. Second, we can obtain more authentic answers by incorporating these additional information. In particular, we observe that we may get incorrect answers if we ignore the constraints. The main reason is derived from ignoring the change of *uncertainty region*¹ and *pdf*.

As an example, see Figure 1, the small black dot denotes the recorded location of the moving object O_j , the radius of circle denotes the distance threshold of O_j , the biggest rectangle R denotes query range, the small rectangle RA_i ($1 \leq i \leq 4$) denotes barrier, we assume O_j cannot reach at the interior of these barriers, it is as similar as taxis cannot run in lakes (or buildings, etc.). For ease of discussion, we assume O_j is subjected to uniform distribution in its uncertainty region, and we term the uncertainty region of O_j as UR_j . Then, the probability of O_j locating in R is equal to the ratio of two areas (i.e., the area of $UR_j \cap R$ and the area of UR_j , where $UR_j \cap R$ denotes the intersection set between UR_j and R).

Given a query “retrieving the objects that are currently locating in R with a non-zero probability”. Figure 1(a) depicts the case ignoring the constraints, where the circle ($O_j \odot$ for short) illustrates the *uncertainty region*. In this case, the query answer will be $\{ (O_1, =100\%), (O_3, >50\%), (O_4, <50\%) \}$, where “<50%” denotes a specific decimal that is large than 0 and less than 0.5, other symbols have similar meanings. In contrast, Figure 1(b) presents the case considering constraints, where $O_j \odot$ can not be simply took as the *uncertainty region* of O_j , the real UR_j is the region that $O_j \odot$ subtracts the *barrier region*, e.g., $UR_3 = (O_3 \odot - RA_3)$. In this case, the query answer will be $\{ (O_1, =100\%),$

¹ The uncertainty region is so called closed region in which the object can be always found, it can be derived based on recorded location and distance threshold.

$(O_3, <50\%), (O_4, >50\%)$. We observe that the above two answers are different, and it is not difficult to find out that the first answer is an incorrect answer.

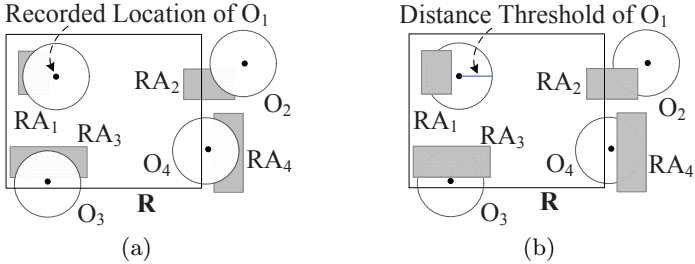


Fig. 1. Illustration of PRQ over uncertain moving objects

Motivated by the above fact, in this paper, we investigate the problem of PRQ over uncertain moving objects in constrained 2D space. To the best of our knowledge, this is the first effort to address this problem. We present our solution for answering this kind of query, the proposed approach is simple and easily to implement, but without loss of efficiency and effectiveness, it can be easily extended to the real applications. Simply speaking, we use polygons to represent restricted areas, and we approximate non-polygon entities (e.g., $O_j \cdot \odot$) to polygons, we utilize tactfully MBRs of various entities to help us pick out useful candidate entities. In order to improve the search efficiency, we use classical R-tree to index, and discuss two R-tree based indexing schemes. We present a label based data structure that is convenient for representing uncertainty region as well as other related entities (e.g., IS_j), at the same time, it contributes to the follow-up calculation. By well analysing the geometry relation between different entities, we design elegant algorithms for computing the uncertainty region and the intersection (between uncertainty region and query range). For obtaining the probability, we present two methods, quick method and Monte Carlo method, for different types of *pdf*. Experiment results demonstrate that our solution is very efficient and effective. To summarize, we make the following contributions.

- We refine primitive uncertain moving object model by introducing the concept of restricted areas, and re-formulate traditional query based on the refined model.
- We, by well analysing the nature of our problem, devise a framework and detailed algorithms for achieving our goals.
- We demonstrate the performance of our proposed methods through extensive experiments under different experiment settings.

The rest of the paper is organized as follows. In successive section, we formalize the problem. We introduce the preliminaries and analyse the nature of some vital entities in section 3. We present the query processing framework and detailed algorithms in section 4, and discuss the indexing schemes in section 5.

We evaluate the performance of our proposed methods through extensive experiments in section 6. Section 7 reviews related works. Finally, we conclude this paper and present our future research directions in section 8.

2 Problem Definition

Given a territory with a number M of disjointed restricted areas (RAs), and there are a number N of moving objects (MOs) which are continuous and freely moving in the territory but cannot enter into those RAs. We assume we already stored the last location ² of each MO in the server. In addition, we assume that a MO reports its location to the sever when the deviation between its current location and recorded location is larger than a distance threshold (DT). Formally, we term the *territory* as T (which is a $2D$ space), disjointed *restricted area* as $RA_i(1 \leq i \leq M)$, *moving object* as $O_j(1 \leq j \leq N)$. For O_j , we term the location at an arbitrary instant of time t as $(L_j^t.X, L_j^t.Y)$, last sampling/reporting time as *last*, current time as *now*, specific location at last sampling/reporting time as $(L_j^{last}.X, L_j^{last}.Y)$, distance threshold as DT_j . In addition, we set the following conditions are always satisfied: $(L_j^t.X, L_j^t.Y) \notin \bigcup_{i=1}^M RA_i \wedge (L_j^t.X, L_j^t.Y) \in T - \bigcup_{i=1}^M RA_i \wedge \bigcup_{i=1}^M RA_i \subset T$.

Since the location of a MO is continuously changing, it is unreasonable if we simply use the recorded location as the current location. Essentially, it is uncertain about whereabouts of the specific location at current time. One common model [15, 13, 14, 16–19], for capturing the location uncertainty of a MO, is comprised by two components:

Definition 1. *The **uncertainty region (UR)** of a moving object O_j at an instant of time t , denoted by UR_j^t , is a closed region where O_j can be found.*

Definition 2. *The **uncertainty probability density function** of O_j at time t , denoted by $f_j^t(x, y)$, is a probability density function (pdf) of O_j 's location at an instant of time t , it has the value of 0 if outside UR_j^t .*

Since $f_j^t(x, y)$ is a *pdf*, in theory, it has the property that $\int_{UR_j^t} f_j^t(x, y) dx dy = 1$. In general, the uncertainty region UR_j^t under distance based update policy can be derived by the formula: $UR_j^t = \pi \cdot (DT_j)^2$, where DT_j is the *distance threshold* of O_j , and the centre of UR_j^t is the recorded location. For convenience, we use $O_j.\odot$ to denote this region. The above representation is feasible if there is no any barrier, it can not work once there exist RAs. Therefore, a real uncertainty region for our problem should be as follows.

$$UR_j^t = O_j.\odot - \bigcup_{i=1}^M (RA_i) \quad (1)$$

² In this paper, the terms *last location* and *recorded location* are used interchangeably.

Note that, under this case, in any two different instant of time t_1 and t_2 ($t_1, t_2 \in (\text{last}, \text{now}]$), we have $UR_j^{t_1} = UR_j^{t_2}$, and $f_j^{t_1}(x, y) = f_j^{t_2}(x, y)$. In view of these, we, unless stated otherwise, will use UR_j and $f_j(x, y)$ to denote uncertainty region and *pdf* of O_j , respectively.

Definition 3. A **Probability Range Query (PRQ)** over uncertain moving objects, in the constrained 2D space, returns a series of tuple in form of (O_j, P_j) , where P_j is the nonzero probability of O_j locating in the closed region R .

Specifically, in this paper, we focus on snapshot query rather than continuous query, and we always assume any two MOs can not locate in same location at same instant of time. For convenience, we summarize the main symbols in Table 1.

Table 1. Main symbols used in this paper

Symbols	Description
R	query range
RA_i	the i restricted area
O_j	the j moving object
UR_j	uncertainty region of the j moving object
DT_j	distance threshold of the j moving object
$f_j(x, y)$	<i>pdf</i> of the j moving object
EP_j	the approximated equilateral polygon derived from $O_j \odot$
IS_j	the intersection between R and UR_j
p_j	probability of O_j locating in query range R

3 Preliminaries

3.1 Representation of the basic entities

Since the realistic application environments are vary from place to place, the shapes of RAs should be diversified. Our objective is building a general approach rather than focusing on certain specific environment. In this paper, we use polygon to represent RA. For $O_j \odot$, which is a circle, we approximate it to an equilateral polygon (EP). Generally speaking, we can get more accurate result if we use more equivalent edges. For clearness, we call the EP derived from $O_j \odot$ as EP_j . Note that, we let $O_j \odot$ be the circumscribed circle of EP_j . By doing so, we can assure that the distance, from any point in EP_j to the center, always is less than its' distance threshold DT_j . The reasons we do this transforming are two folds. First, it is convenient for the follow-up calculation since operating on line segments, in most cases, is more simple and efficient than on arcs. Second, it is easy to represent the result of calculation. The method of transforming $O_j \odot$ to EP_j is very simple, we just let $X_k = L_j^{\text{last}} \cdot X + DT_j \cdot \cos((k - 1) \cdot 2\pi/EL)$,

and $Y_k = L_j^{last} \cdot Y + DT_j \cdot \sin((k-1) \cdot 2\pi/EL)$, where EL is the number of edges (of EP_j), $k \in [1, 2, \dots, EL]$, (X_k, Y_k) is the k^{th} vertex of EP_j .

3.2 Notations of geometry relations and operations

Given two arbitrary *simple polygons*³ PA and PB . In general, there are five types of geometry relations: $PA \cap PB$, $PA \subset PB$, $PA \supset PB$, $PA \equiv PB$, $PA \uparrow\uparrow PB$. Where $PA \equiv PB$ means that the two polygons are totally coinciding. $PA \uparrow\uparrow PB$ means that PA and PB are disjointed. The subtraction operation and intersection operation are two common geometry operations, which are used extensively in this paper. For clearness, we use “ $PA - PB$ ” and “ $PA \wp PB$ ” to denote them, respectively.

3.3 Candidate moving objects and candidate restricted areas

For ease of discussion, in the rest of this paper, we use BRA_i to denote the MBR of RA_i , and use $BRA_i.left$, $BRA_i.right$, $BRA_i.top$ and $BRA_i.bottom$ to denote the boundary of BRA_i . Unless stated otherwise, we deal with other MBRs similarly (e.g., we use BEP_j to denote the MBR of EP_j).

Definition 4. *Given a number N of moving objects, their distance thresholds, and a closed region R , we use their MBRs to prune the unrelated moving objects, all moving objects that are not been pruned are the **candidate moving objects (CMOs)**.*

Definition 5. *Given a number M of restricted areas, a moving object O_j and its’ distance threshold, we use their MBRs to prune unrelated restricted areas, all restricted areas that are not been pruned are O_j ’s **candidate restricted areas (CRAs)**.*

3.4 Understanding the UR

Given a number of RAs, generally speaking, there are three types of cases for a MO O_j . (1) There is no RA intersecting with EP_j . (2) That EP_j subtracts all RAs is a single region. (3) That EP_j subtracts all RAs has no less than two subdivisions. As an example, grey polygon denotes RA, black dot denotes O_j , equilateral polygon denotes EP_j ($j \in [1, \dots, 4]$), as shown in Figure 2. Obviously, O_1 belongs to the first class, its’ UR is EP_1 . O_2 and O_3 belong to the second class. For O_2 (or O_3), its’ UR is the result of that EP_2 (or EP_3) subtracts all RAs. O_4 belongs to the third class, that EP_4 subtracts all RAs has two subdivisions, S_1 and S_2 , its’ UR is S_2 . This is because one (from the center point of EP_4) cannot reach any location in S_1 if he do not walk outside the EP_4 . Therefore, S_1 should be discarded.

Note that, there is a *hole* in UR_3 . In here, we give the definition of *hole*, *outer ring*, *inner ring*.

³ In here, a *simple polygon*, we mean it is not self-intersection, and there is no *hole(s)* in it.

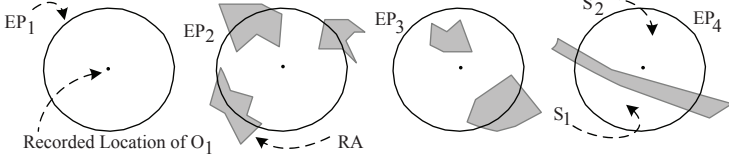


Fig. 2. Illustration of UR

Definition 6. Given three closed region R_1, R_2, R_3 , in which $R_1 \subset R_2$ and $R_3 = R_2 - R_1$. Then, we call the periphery of R_2 and that of R_1 as the closed region R_3 's **outer ring** and **inner ring**, respectively, and we call the region surrounded by R_3 's inner ring as a **hole** of R_3 .

3.5 Understanding the IS

Let UR_j is a closed region with k (≥ 0) holes, query range R is a closed region. The intersection (IS) between R and UR_j can be parsed by understanding the relation between R and the *outer ring* (or *inner ring(s)*) of UR_j . For ease of discussion, we term the IS between UR_j and R as IS_j , the outer ring of UR_j as OUR_j , and call the i^{th} inner ring (or hole) of UR_j as IUR_j^i ($i \leq k$). The geometry relation between OUR_j and R has 5 cases as shown in “Box Graph 1”.

case 1.	$OUR_j \uparrow\uparrow R$	$\rightarrow IS_j = \emptyset$.
case 2.	$OUR_j \subset R$	$\rightarrow IS_j = UR_j$.
case 3.	$OUR_j \equiv R$	$\rightarrow IS_j = UR_j$.
case 4.	$OUR_j \supset R$	
case 4.1.	$k = 0$	$\rightarrow IS_j = R$.
case 4.2.	$k \neq 0$	$\rightarrow IS_j = R - \sum_{i=1}^k IUR_j^i$.
case 5.	$OUR_j \cap R$	
case 5.1.	$k = 0$	$\rightarrow IS_j = OUR_j \overset{\circ}{\cap} R$.
case 5.2.	$k \neq 0$	$\rightarrow IS_j = (OUR_j \overset{\circ}{\cap} R) - \sum_{i=1}^k IUR_j^i$.

Box Graph 1

case 4.2.1.	$R \equiv IUR_j^i$	$\rightarrow IS_j = \emptyset$.
case 4.2.2.	$R \subset IUR_j^i$	$\rightarrow IS_j = \emptyset$.
case 4.2.3.	$R \uparrow\uparrow IUR_j^i$	$\rightarrow IUR_j^i$ make no any impact on IS_j .
case 4.2.4.	$R \supset IUR_j^i$	$\rightarrow IUR_j^i$ will be a hole of IS_j .
case 4.2.5.	$R \cap IUR_j^i$	$\rightarrow IUR_j^i$ possible subdivide R .

Box Graph 2

case 5.2.1.	$OcR \uparrow\uparrow IUR_j^i$	$\rightarrow IUR_j^i$ make no any impact on IS_j .
case 5.2.2.	$OcR \supset IUR_j^i$	$\rightarrow IUR_j^i$ will be a hole of IS_j .
case 5.2.3.	$OcR \cap IUR_j^i$	$\rightarrow IUR_j^i$ possible subdivide OcR .

Box Graph 3

In the sequel, we mainly discuss case 4.2 and case 5.2 since other cases are straightforward. For case 4.2, the geometry relation between R and IUR_j^i also has 5 cases as shown in “Box Graph 2”.

Note that, for case 4.2.5, given R is subdivided, by certain hole (e.g., IUR_j^1), into two subdivisions, say S_1 and S_2 . Next, S_1 (or S_2) possible will be further subdivided, by another hole (e.g., IUR_j^2), into two subdivisions $S_{1,1}$ and $S_{1,2}$ ($S_{2,1}$ and $S_{2,2}$), and so on. For case 5.2, we should consider the impact of IUR_j^i on “ $OUR_j \setminus R$ ”, we substitute “ $OUR_j \setminus R$ ” with “ OcR ” for convenience, there are 3 cases as shown in “Box Graph 3”.

For case 5.2.3, it is similar to case 4.2.5, given OcR is subdivided, by certain hole (e.g., IUR_j^1) into two subdivisions S_1 and S_2 . Next, S_1 (or S_2) possible be further subdivided by other hole (e.g., IUR_j^2).

3.6 Label based data structure

We observe that, UR may be a closed region with hole(s) or may just be a simple closed region. In addition, IS possible consists of multiple subdivisions with hole(s). For ease of operating on them in an unified manner, we present a label based data structure (LBDS), which consists of three domains, one *label* domain and two *pointer* domains.

- Flag: the function of this domain is to tell us whether there is/are hole(s) in the entity. Specifically, when *Flag* is equal to 0, it means that there is no hole in it. Otherwise, there is no less than one hole.
- OPointer: this domain points to a simple polygon, which denotes the outer ring of the entity. A simple polygon consists of five domains.
 - VPointer: this domain points to a linked list in which a series of vertexes are stored.
 - left: the left boundary of this polygon.
 - right: the right boundary of this polygon.
 - top: the top boundary of this polygon.
 - bottom: the bottom boundary of this polygon.
- IPointer: this domain points to a linked list in which the simple polygon(s) is/are stored if *Flag* is not equal to 0, in here the simple polygon(s) denotes the inner ring(s)/hole(s) of this entity.

The UR can be represented directly by the LBDS, the IS can be represented by a linked list in which a series of ‘LBDS’ are stored.

4 Query Evaluation

4.1 The Framework

Figure 3 illustrates the pseudocode of the basic framework for answering PRQ over uncertain moving object in constrained 2D space. Specifically, there are several steps. First, we search the CMOs, which can be achieved by comparing

their MBRs (line 2). Second, for each CMO, we search its' CRAs, and compute its' UR and IS (line 4-6). Third, if the IS is equal to the UR (or \emptyset), we assign the probability P_j with 1 (or 0). Otherwise, we obtain the probability by calculating the integral on IS (line 7-9). Fourth, if the P_j is not equal to 0, we store the 'identity' of this CMO and its' probability, then shift to dealing with next CMO until all CMOs have been processed (line 10). At last, returning the result in which all CMOs that have non-zero probability are included (line 11).

```

Procedure QueryFramework {
  Input:  $R, (L_j^{last}.X, L_j^{last}.Y), DT_j, RA_i, f_j(x, y)$ 
  Output:  $\cup(O_j, P_j)$ , where  $P_j > 0$ 
  (1)  $Answers \leftarrow \emptyset$ ;
  (2) CMOs  $\leftarrow$  the moving objects that may locate in  $R$ 
  (3) for each  $O_j \in$  CMOs
  (4)   CRAs  $\leftarrow$  searching candidate restricted areas
  (5)    $UR_j \leftarrow$  computing the uncertainty region of  $O_j$ 
  (6)    $IS_j \leftarrow$  computing  $UR_j \cap R$ 
  (7)   if ( $IS_j \neq \emptyset$ )
  (8)     if ( $IS_j = UR_j$ ) then  $P_j \leftarrow 1$ 
  (9)     else  $P_j \leftarrow \int_{IS_j} f_j(x, y) dx dy$ 
  (10)  if ( $P_j \neq 0$ ) then  $Answers \leftarrow (O_j, P_j) \cup Answers$ 
  (11) return  $Answers$  }

```

Fig. 3. PRQ over Uncertain Moving Objects in Constrained 2D Space

Note that, there are two issues we should well consider in this framework. (1) Evaluating UR can not been took as simple “polygon-polygon subtraction”, existing algorithm (e.g., [26]) only is the basis of this work. (2) Computing IS also is not simple “polygon-polygon intersection”, existing algorithms (e.g., [27–30]), which support “intersection operation” on polygons with holes, but do not well consider the case where a large number of holes possible exist, and do not well consider that a subdivision possible be continuously subdivided. Moreover, it is very frequent to compute UR and IS in our query processing. Therefore, it is very necessary to consider the nature of this problem, then, to devise targeted algorithms.

4.2 Computing the UR

In this Subsection, we present our approach for computing the UR. We first address the tactics, and followed by presenting the detailed procedure. On the whole, we take use of four tactics. (1) We deal with the CRA that may result in multiple subdivisions to the entity (e.g., EP_j) as early as possible. (2) Once multiple subdivisions appear, we update immediately the boundary, i.e., MBR. Otherwise, we do not update the boundary before we traversed all the CRAs. (3) Once we confirm the entity has ever been subdivided, we use the new boundary to prune the rest of CRAs. (4) We process the CRA that results in holes to current entity as late as possible.

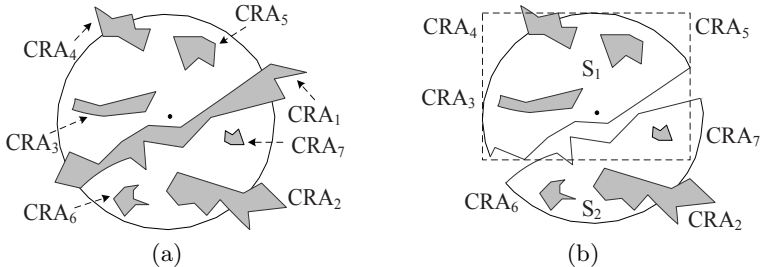


Fig. 4. Illustration of Computing UR

4.2.1 The span of CRA

Given O_j has a number k of CRAs (CRA_1, \dots, CRA_k). For obtaining the UR_j , a direct method is evaluating the subtraction between EP_j and all the CRAs one by one. However, it is a brute force solution. For illustrating the reason, we first give the definition of *vertical span*, *horizontal span* and *span*.

Definition 7. Given RA_i and BRA_i , the **horizontal span** of RA_i is $|BRA_i.right - BRA_i.left|$, $RA_i.HS$ for short. Similarly, the **vertical span** of RA_i is $|BRA_i.top - BRA_i.bottom|$, $RA_i.VS$ for short. The **span** of RA_i is $MAX\{RA_i.HS, RA_i.VS\}$.

For CRA_m and CRA_n ($m, n \in [1, \dots, k]$, $m \neq n$), their *spans* may be different. In particular, we observe that a CRA with large span is more likely subdivide a single region into two (or more) subdivisions than a CRA with small *span* is. This observation will contribute to the evaluation of UR_j . In here, we sort all the CRAs of O_j , according to their spans, in descending order before evaluating the subtraction between EP_j and CRAs. As an example, see Figure 4, the big equilateral polygon denotes the EP_j , grey polygon denotes candidate restricted area CRA_m ($m \in [1, \dots, 7]$), and given their spans are decreasing from CRA_1 to CRA_7 . Therefore, based on our tactics, we should deal with CRA_1 at first, then deal with CRA_2 , and so on. Note that, after we deal with CRA_1 , there are two subdivisions, S_1 and S_2 , as shown in Figure 4(b). Based on the analysis in Subsection 3.4, we choose S_1 as the real subdivision. Thus, when we deal with CRA_2 , we can determine quickly that it is irrelevant with the final result. Otherwise, if we deal with CRA_2 before we deal with CRA_1 , then we have to compute “ $EP_j - CRA_2$ ”, which will incur extra cost.

4.2.2 Tactic for handling hole

Given we have sorted all the CRAs of O_j . Next, we can evaluate the subtraction between EP_j and CRAs one by one. For clearness, we call the result of “ $EP_j - CRA_1$ ” as $EP_j.1$, the result of “ $EP_j.1 - CRA_2$ ” as $EP_j.2$, and so on. Note that, we use EP_j and “ $EP_j.0$ ” interchangeably. In some cases, $CRA_m \subset EP_j.(m-1)$ ($m \in [1, \dots, k]$). Obviously, CRA_m in this time results in a hole to the current $EP_j.(m-1)$. A straightforward method is computing “ $EP_j.(m-1) - CRA_m$ ” and updating the $EP_j.(m-1)$ right now, and then to deal with the next CRA using the new $EP_j.m$. However, we observe that

doing in this manner will make the follow-up calculation complicate. In here, we postpone the subtraction operation if CRA_m results in a hole to the current $EP_j.(m-1)$. Specifically, we store CRA_m in another place and deal with it after we traversed all the rest of CRAs of O_j . Taking CRA_3 in Figure 4(b) as an example, it results in a hole to $EP_j.2$, we store it in another place (e.g., a linked list 'uHoles'), and shift to dealing with CRA_4 , and so on. After we traversed all the rest of CRAs of O_j , we fetch CRA_3 from the linked list 'uHoles', and to determine whether it results in a hole to $EP_j.7$. In here, it is, so we put it as an inner ring of $EP_j.7$.

4.2.3 Updating regulations

As stated above, the EP_j is continuous evolving in the process of computing UR. If " $CRA_m \cap EP_j.(m-1)$ ", then, the value of $EP_j.(m-1)$ should be different from that of " $EP_j.(m-1) - CRA_m$ ". In this case, we update by assigning the result of " $EP_j.(m-1) - CRA_m$ " to $EP_j.m$. Correspondingly, the $BEP_j.m$, i.e., MBR of $EP_j.m$, may be changed. In principle, once it is true, we should compute the new MBR and assign it to $BEP_j.m$. However, we do not update the MBR right now, since we observe that, in most cases, the new MBR should not make enough contribution to the rest of computation. In addition, if we manage to compute the new MBR, we have to traverse the vertexes of $EP_j.m$, which will take a few of time. In here, we update the MBR in a lazy manner. Specifically, we update the MBR only in two cases: either CRA_m subdividing $EP_j.(m-1)$ into no less than 2 subdivisions, or having traversed all the CRAs of O_j . Taking CRA_1 in Figure 4 as an example, after we dealt with it, two subdivisions are presented, in this time, we should update EP_j and BEP_j . Specifically, we assign S_1 to $EP_j.1$, and assign the MBR of S_1 to $BEP_j.1$. For CRA_2 and CRA_3 , " $CRA_2 \uparrow\uparrow EP_j.1$ " and " $CRA_3 \subset EP_j.2$ ", thus, we let $EP_j.2 = EP_j.1$ and $EP_j.3 = EP_j.2$ according to our tactic. That is, there is no any update when we deal with CRA_2 and CRA_3 . For CRA_4 , we let $EP_j.4 = EP_j.3 - CRA_4$, that is, we update $EP_j.3$. However, we do not update $BEP_j.3$ whatever the real MBR of " $EP_j.3 - CRA_4$ " is, since " $EP_j.3 - CRA_4$ " does not result in multiple subdivisions. So we let $BEP_j.4 = BEP_j.3$.

4.2.4 The new boundary

As previous discussion, we update the boundary when a CRA subdivides current entity, the new boundary will contribute to pruning the rest of unrelated CRAs. In here, we use a 'switch' to remember whether the entity has ever been subdivided. Once the 'switch' is set to 1, in the rest of computation, we always compare their MBRs before evaluating the subtraction. For example, the dashed rectangle in Figure 4(b) is the new boundary after we dealt with CRA_1 , thus, for the rest of CRAs (from CRA_2 to CRA_7), we always use the new boundary to determine whether certain CRA can be pruned directly. In here, both CRA_2 and CRA_6 can be pruned directly. Note that, if the 'switch' is off (i.e., 0), we never compare their MBRs since it doubtlessly incurs cost but without any benefit in terms of the rest of computation.

```

Procedure EvaluateUR ( ) {
  Input: ( $L_j^{last}.X$ ,  $L_j^{last}.Y$ ),  $DT_j$ ,  $\sum_{i=1}^M RA_i$ 
  Output:  $UR_j$ 
  (1)  $UR_j \leftarrow \emptyset$ ;  $EP_j \leftarrow \text{Transform } O_j \odot$ ;  $BEP_j \leftarrow \text{MBR of } EP_j$ 
  (2) CRAs  $\leftarrow$  search candidate restricted areas based on  $BEP_j$  and  $BRA_i$ 
  (3) if (CRAs  $\neq \emptyset$ )
  (4)   sorting CRAs;  $switch \leftarrow 0$ ;  $uHoles \leftarrow \emptyset$ ;  $rHoles \leftarrow \emptyset$ 
  (5)   for each candidate restricted area  $CRA_m \in \text{CRAs}$ 
  (6)     if ( $switch = 0$ ) then Procedure HandleCRA ( $uHoles, CRA_m, switch, EP_j$ )
  (7)     else //  $switch = 1$ 
  (8)       if ( $\neg(BCRA_m \uparrow\uparrow BEP_j)$ ) then
  (9)         Procedure HandleCRA( $uHoles, CRA_m, switch, EP_j$ )
  (10)  if ( $uHoles \neq \emptyset$ ) then
  (11)    for each  $CRA_m \in uHoles$ 
  (12)      if ((vertex of  $CRA_m$ )  $\in EP_j$ ) then  $rHoles = rHoles \cup CRA_m$ 
  (13)      if ( $rHoles \neq \emptyset$ ) then Let all CRAs ( $\in rHoles$ ) as the inner ring of  $EP_j$ 
  (14)  $UR_j \leftarrow EP_j$ ;
  (15) return  $UR_j$  }
  Procedure HandleCRA ( ) {
  Input:  $EP_j$ ,  $CRA_m$ ,  $uHoles$ ,  $switch$ 
  (16) if ( $EP_j \cap CRA_m$ )
  (17)    $EP_j \leftarrow EP_j - CRA_m$ ;  $SN \leftarrow$  number of subdivisions in  $EP_j$ 
  (18)   if ( $SN > 1$ ) then
  (19)      $EP_j \leftarrow$  choose real subdivision from multiple subdivisions; update  $BEP_j$ 
  (20)     if ( $switch = 0$ ) then  $switch \leftarrow 1$ 
  (21) else // ( $EP_j \supset CRA_m$ ) or ( $EP_j \uparrow\uparrow CRA_m$ )
  (22)   if ( $EP_j \supset CRA_m$ ) then  $uHoles \leftarrow uHoles \cup CRA_m$  }

```

Fig. 5. Pseudocode for Computing UR

4.2.5 The procedure for computing UR

Figure 5 depicts the pseudocode of computing UR, which consists of two procedures: `HandRA()` and `EvaluateUR()`. Note that, some symbols (e.g., EP_j) used in the two procedures should be understood as similar as our previous discussion since these entities are evolving continuously.

Procedure EvaluateUR() First we get the CRAs of O_j based on the MBRs (line 1-2). If CRAs $\neq \emptyset$, we sort CRAs and initialize (line 4), where $switch$ is used for indicating whether the EP_j has ever been subdivided, $uHoles$ is used for storing the CRA that results in hole to current EP_j , $rHoles$ is used for storing the CRA ($\in uHoles$) that results in hole to the last EP_j . Since we adopt lazy updating manner, once BEP_j is updated, we should use the new MBR to determine whether a CRA can be pruned before dealing with it, otherwise, we deal with it directly using the procedure `HandCRA()` (line 6-9). Once we traversed all CRAs, we determine whether the CRA ($\in uHoles$) results in hole to the last EP_j , which can be achieved by determining “whether vertex from CRA locates in the last EP_j ”. In here, we use Hormann et al. [31] proposed algorithm to process the *point in polygon problem*. All the CRAs ($\in rHoles$) will be as the *inner ring* of the last EP_j . In the end, we assign the last EP_j to UR_j (line 10-15).

Procedure HandCRA() First we determine the geometry relation between the current EP_j and the CRA. There are 3 cases. For $EP_j \cap CRA$, we use Margalit et al.[26] proposed algorithm to do subtraction operation. For $EP_j \supset CRA$, we add the CRA into $uHoles$ linked list, and do nothing when $EP_j \uparrow\uparrow CRA$.

4.3 Computing the IS

In Section 3, we have well analysed the IS according to the geometry-topological relation between R and the outer ring (or inner ring) of UR, which is the basis of developing the targeted algorithm for computing IS.

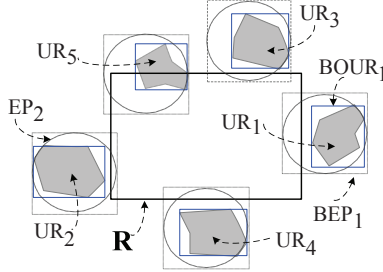


Fig. 6. Illustration of the first level screening

4.3.1 Multi-levels screening

For get the IS_j , we use tactfully the MBRs to do elementary screening before executing geometry operation on two entities. The first level screening is for OUR_j and R , we call their MBRs as $BOUR_j$ and BR , respectively. Obviously, if $BOUR_j \uparrow\uparrow BR$, the IS_j must be \emptyset . As an example, the biggest rectangle illustrates query range R as shown in Figure 6, it has 5 CMOs since $BR \cap BEP_j$ ($j \in [1, \dots, 5]$), the grey polygons illustrate their URs. In order to evaluate the IS_j , first, we execute the first level screening. In here, $BR \uparrow\uparrow BOUR_j$ ($1 \leq j \leq 4$), therefore, we can know immediately that the IS_j is equal to 0. Note that, for UR_5 , we cannot pruned quickly by the first level screening.

The second level screening help us find out candidate holes (*cHoles* for short) from $\sum_{i=1}^k IUR_j^i$. There are two cases: (1) using MBR of R to prune unrelated holes. As an example, the black solid line rectangle in Figure 7(a) illustrates query range R , the grey region is UR_1 which has 7 holes (the white polygons), say IUR_1^i ($i \in [1, \dots, 7]$). In here, $R \subset OUR_1$, therefore, the $IS_1 = R - \sum_{i=1}^7 IUR_1^i$ (recall case 4.2 in Subsection 3.4). In here, IUR_1^1 and IUR_1^2 can be pruned by the second level screening, the rest of holes are the candidate holes. (2) using MBR of OcR ($OUR_j \setminus R$) to prune unrelated holes. Figure 7(b) presents this case, in here, $R \cap OUR_1$, therefore, the $IS_1 = (R \setminus OUR_1) - \sum_{i=1}^7 IUR_1^i$ (recall case 5.2 in Subsection 3.4). Similar to previous case, in here, IUR_1^1 and IUR_1^2 can be pruned by the second level screening.

The third level screening is using the MBR of candidate hole to prune unrelated subdivisions. There also are two cases: (1) the subdivisions are derived from R . As an example, given we deal with the candidate holes in Figure 7(a) from left to right. So we deal with IUR_1^6 at first, note that, " $R - IUR_1^6$ " has two subdivisions, S_1 and S_2 , as shown in Figure 7(c). Next, when we deal with IUR_1^5 , we

use the MBR of IUR_1^5 to prune unrelated subdivision. In here, $BS_1 \uparrow\uparrow BIUR_1^5$, so S_1 is pruned. Similarly, after we dealt with IUR_1^7 , S_2 is subdivided into $S_{2,1}$ and $S_{2,2}$, as shown in Figure 7(d). So when we deal with IUR_1^3 (or IUR_1^4), S_1 and $S_{2,1}$ can be pruned. (2) the subdivisions are derived from OcR . For example, after we deal IUR_1^6 in Figure 7(b), OcR will be subdivided into two subdivisions, for the rest of candidate holes, we always use the MBR of candidate hole to prune unrelated subdivisions.

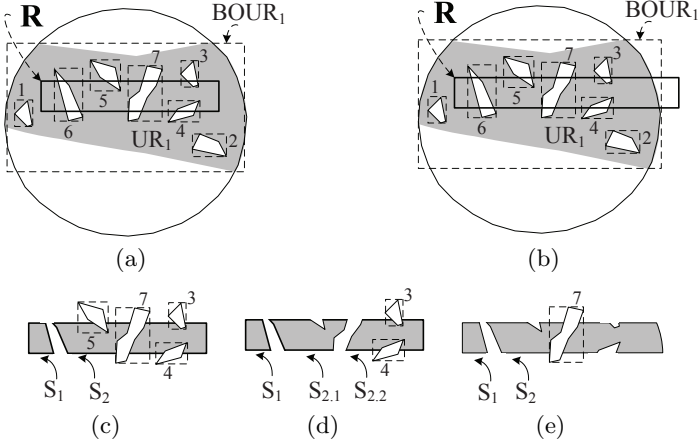


Fig. 7. Illustration of Computing IS

4.3.2 Sorting candidate holes in ascending order

Similar to CRA, a candidate hole with large span also is more likely subdivide a single region into two (or more) subdivisions than a hole with small span is. In Subsection 4.2.1, we deal with CRA with large span as early as possible. On the contrary, we, in here, deal with candidate hole with large span as late as possible. So we sort them in ascending order rather than in descending order, before we execute geometry operation on them. The reason is that the new produced subdivisions can not be discarded, and should be used when we deal with the rest of candidate holes. If we deal with candidate hole with large span at first, it is possible that many subdivisions were produced before we deal with other candidate holes with small spans, which will incur more cost to compare the MBRs. As an example, let's revisit Figure 7(b), there are 5 candidate holes, say IUR_1^i ($i \in [3, \dots, 7]$), given their spans are increasing from IUR_1^3 to IUR_1^7 . Then, according to our tactic, we should deal with IUR_1^3 at first, next, deal with IUR_1^4 , and so on. Figure 7(e) illustrates the situation after we dealt with the IUR_1^6 , there are two subdivisions, S_1 and S_2 . So when we deal with IUR_1^7 , the third level screening (recall Subsection 4.3.1) are activated since there are multiple subdivisions. Note that, in here we only execute two times comparison, i.e., we compare the MBR of IUR_1^7 with the MBR of S_1 , and with the MBR

```

Procedure EvaluateIS ( ) {
  Input:  $UR_j, R$ 
  Output:  $IS_j$ 
  (1)  $IS_j \leftarrow \emptyset$ ;
  (2) if  $(\neg(BUR_j \uparrow\uparrow BR))$  then
  (3)   if  $((UR_j.Flag = 1) \wedge ((OUR_j \supset R) \vee (OUR_j \cap R)))$  then
  (4)     if  $(OUR_j \supset R)$  then // case 4.2
  (5)        $tempIS \leftarrow R$ ;
  (6)     else //  $OUR_j \cap R$ , case 5.2
  (7)        $tempIS \leftarrow OcR$ ; //  $OcR = OUR_j \setminus R$ 
  (8)     Procedure HandleComplex ( $tempIS, UR_j$ );
  (9)      $IS_j \leftarrow tempIS$ ;
  (10)  else // other cases are straightforward
  (11)   $IS_j \leftarrow$  “certain value” ; // please refer to Subsection 3.5
  (12) return  $IS_j$  }

Procedure HandleComplex ( ) {
  Input:  $tempIS, UR_j$ 
  (13)  $cHoles \leftarrow \emptyset$ ;  $rHoles \leftarrow \emptyset$ ;  $sign \leftarrow 0$ 
  (14) for each  $hole_i \in UR_j$ 
  (15)   if  $(\neg(Bhole_i \uparrow\uparrow BtempIS))$  then    $cHoles \leftarrow cHoles \cup hole_i$ 
  (16)   sort  $cHoles$  based on  $span$ ;
  (17) for each  $hole_i \in cHoles$ 
  (18)   if  $(sign = 0)$  then
  (19)     if  $(tempIS \equiv hole_i \vee tempIS \subset hole_i)$  then  $tempIS \leftarrow \emptyset$ ; return ;
  (20)     else if  $(tempIS \supset hole_i)$  then  $rHoles \leftarrow rHoles \cup hole_i$ ;
  (21)     else if  $(tempIS \uparrow\uparrow hole_i)$  then // do nothing
  (22)     else //  $(tempIS \cap hole_i)$ 
  (23)        $tempIS \leftarrow tempIS - hole_i$ ;  $NS \leftarrow$  number of subdivisions in  $tempIS$ ;
  (24)       if  $(NS > 1)$  then  $sign \leftarrow 1$ 
  (25)     else //  $(sign = 1)$ 
  (26)        $temp \leftarrow \emptyset$ 
  (27)       for each subdivision  $S_i$  ( $\in tempIS$ )
  (28)         if  $(\neg(Bhole_i \uparrow\uparrow BS_i))$  then
  (29)           if  $(S_i \cap hole_i)$  then
  (30)              $temp \leftarrow temp \cup (S_i - hole_i)$ ; delete  $S_i$  from  $tempIS$ 
  (31)           else if  $(S_i \supset hole_i)$  then  $rHoles \leftarrow rHoles \cup hole_i$ ; break;
  (32)           else //  $(S_i \uparrow\uparrow hole_i)$ , do nothing
  (33)            $tempIS \leftarrow tempIS \cup temp$ 
  (34) if  $(rHoles \neq \emptyset)$  then
  (35)   for each  $hole_i \in rHoles$ 
  (36)     for each  $S_i \in tempIS$ 
  (37)       if  $((vertex\ of\ hole_i) \in S_i)$  then
  (38)         let  $hole_i$  as an inner ring of  $S_i$ ; break; }

```

Fig. 8. Pseudocode of Computing IS

of S_2 . However, the times of comparison in Figure 7(c) and 7(d), where we deal with candidate holes from left to right, it takes 10 times comparison.

4.3.3 Other tactics

Similar to discussion in Subsection 4.2, once an single region is subdivided, we update the boundary, but there is a little difference. We use the new produced “multiple” subdivisions to substitute the old “single” region, and update the boundary of “each” new subdivision. Otherwise, we postpone updating the boundary. In addition, the tactic for dealing with entities that may result in hole is as same as that in Subsection 4.2.2.

4.3.4 Procedure for Computing IS

Figure 8 depicts the pseudocode of computing IS, which consists of 2 procedures.

Procedure EvaluateIS() First, we use the MBRs of R and OUR_j to validate if they are disjointed, i.e., the first level screening. Otherwise, we, based on their geometry relation and $UR_j.Flag$, do different processing. Note that, we just list the *case 4.2* and *case 5.2* for saving space, other *cases* are very simple, which can be extended in a straightforward manner (refer to Subsection 3.5).

Procedure HandleComplex() This procedure is used for dealing with *case 4.2* and *case 5.2*. First, we obtain the candidate holes, i.e., the second level screening, and sort them based on their spans (line 13-16). Next, we process each candidate hole (line 17-33). If the entity '*tempIS*' has not ever been subdivided by candidate hole, we execute the line 18-24. Otherwise, we execute line 25-33. In here, we use MBR of $hole_i$ and MBR of S_i to prune unrelated subdivision (line 28), i.e., the third level screening.

Note that, We add the result of " $S_i - hole_i$ " into *temp* and delete S_i from *tempIS* (line 30), where *temp* is a linked list that store the modified S_i (i.e., " $S_i - hole_i$ "), this is because the current hole will not make any impact on the modified (or new) S_i . Therefore, we store the modified S_i in *temp* for the present, and we combine the *temp* and *tempIS* until we traversed all old S_i (line 33). In addition, when $S_i \supset hole_i$, we postpone dealing with this hole by storing $hole_i$ into *rHoles* (line 31), where *rHoles* is linked list used for storing $hole_i (\in cHoles)$ that must be a hole in IS_j . At last, if *rHoles* is not empty, we put all the holes ($\in rHoles$) into their corresponding subdivision (line 34-38).

4.4 Evaluation of Probability

In this Subsection, we address two methods for evaluating the probability, one for uniform distribution *pdf*, another is for arbitrary distribution *pdf*.

4.4.1 Quick Method

In here, we present the quick method, which is simple and efficient for uniform distribution *pdf*. As Pfoerster et al. [12] pointed out, uniform distribution corresponds to the "worst-case" scenario. In this case, $f_j(x, y) = 1/AUR_j$, where AUR_j is the area of UR_j . For clearness, we call the area of IS_j as AIS_j , then, we have $P_j = AIS_j/AUR_j$. Therefore, the crucial task is to evaluate AUR_j and AIS_j . Our data representation, LBDS (recall Subsection 3.6), has a great advantage on evaluating their areas, since we use polygon as a basic element, the area of a polygon can be derived based on the following formula.

$$S = \frac{1}{2} \cdot \left(\left| \begin{array}{cc} x_1 & x_2 \\ y_1 & y_2 \end{array} \right| + \left| \begin{array}{cc} x_2 & x_3 \\ y_2 & y_3 \end{array} \right| + \dots + \left| \begin{array}{cc} x_n & x_1 \\ y_n & y_1 \end{array} \right| \right) \quad (2)$$

where $\left| \begin{array}{cc} x_1 & x_2 \\ y_1 & y_2 \end{array} \right| = (x_1 \cdot y_2 - x_2 \cdot y_1)$, and (x_1, y_1) denotes a vertex, other symbols have similar meanings. Therefore, both the AUR_j and AIS_j can be easily obtained. Specifically, we can get the AUR_j based on the following formula.

$$AUR_j = AOUR_j - \sum_{i=0}^K AIUR_j^i \quad (3)$$

where $AOUR_j$ is the area of OUR_j , $K (\geq 0)$ is the number of *holes* in UR_j , $AIUR_j^i$ is the area of the i^{th} hole in UR_j , $i \leq K$. Similarly, For AIS_j , we have

$$AIS_j = \sum_{i=1}^{NS} AS_i = \sum_{i=1}^{NS} (AOS_i - \sum_{k=0}^K AIS_i^k) \quad (4)$$

where $NS (\geq 1)$ is the number of subdivisions in IS_j , AS_i is the area of the i^{th} subdivision, AOS_i is the area of outer ring from S_i , $K (\geq 0)$ is the number of holes in S_i , AIS_i^k is the area of the k^{th} hole from S_i , $k \leq K$.

4.4.2 Monte Carlo Method

When the *pdf* is not uniform distribution, we have to utilize other methods in order to get the P_j . In general, numerical integration is a desired choice. We adopt Monte Carlo (MC) method for achieving this goal. The pseudocode of MC method is illustrated in Figure 9.

Simply to speaking, there are 4 steps. (1) We generate repeatedly random points in the MBR of UR_j until the number of *valid random point* is equal to a pre-set value (N_{seed} for convenience). (2) For each random generated point, we validate whether or not it is locating in UR_j . Note that, we should differentiate if there is hole in UR_j . We take a random point as a *valid random point* only if the point is indeed locating in UR_j . (3) If it is *valid random point*, we, based on the coordinate of *valid random point* and the *pdf*, evaluate the value of $f_j(x_i, y_i)$. Meanwhile, we accumulate this value to a variable (SUM_1 for convenience). In addition, we validate whether or not it also is locating in IS_j . If so, we also accumulate this value to another variable (SUM_2 for convenience). (4) we compute SUM_2/SUM_1 when the number of *valid random point* is equal to N_{seed} , and assign the value to P_j .

```

Procedure MonteCarlo ( ) {
  Input:  $UR_j, IS_j, N_{seed}$ 
  Output:  $P_j$ 
  (1)  $P_j \leftarrow 0, SUM_1 \leftarrow 0, SUM_2 \leftarrow 0, N_1 \leftarrow 0$ 
  (2) repeat
  (3)    $Pt_i \leftarrow$ generate a random point in the MBR of  $UR_j$ 
  (4)   if ( $Pt_i$  locates in  $OUR_j$ ) then
  (5)     if ( $UR_j.Flag = 1$ ) then  $sign \leftarrow 0$ 
  (6)     for each hole in  $UR_j$ 
  (7)       if ( $Pt_i$  locating in hole) then  $sign \leftarrow 1$ ; break;
  (8)     if ( $sgin=1$ ) then continue; //shift to generate next random point
  (9)      $SUM_1 \leftarrow SUM_1 + f_j(x_i, y_i); N_1 \leftarrow N_1 + 1$ 
  (10)    for each  $IS_j^i \in IS_j$ 
  (11)      if ( $Pt_i$  locates in  $OIS_j^i$ ) then  $SUM_2 \leftarrow SUM_2 + f_j(x_i, y_i)$ 
  (12) until  $N_1 = N_{seed}$ 
  (13)  $P_j \leftarrow (SUM_2/SUM_1)$ 
  (14) return  $P_j$  }

```

Fig. 9. Psuedocode of MC Method for Computing P_j

5 Indexing Schemes

It can work correctly using the proposed approaches. However, there still is a considerable space for improvement. In Section 4, we use MBRs to determine CMOs and CRAs. However, the manner to prune unrelated moving objects and restricted areas is one-by-one. It is low efficiency once M and/or N increases. In here, we adopt classical R-tree to index. There are two schemes even if we choose R-tree to index.

5.1 Immediate indexing

Since all RAs are static, their MBRs can be obtained easily. In addition, since we already stored location and distance threshold of MO in database, the MBRs of all MOs also can be easily computed. Therefore, for all RAs and MOs, we can index immediately them based on their MBRs. Once we finish indexing on all RAs and MOs, then, we can, using the two indices, quickly prune unrelated RAs and MOs, respectively. If a MO reports its' new location to database server, we update database record and location index. Note that, there are two indices that one is for indexing RAs, another is for indexing the locations of MOs (by incorporating distance threshold). We can construct the two indices in concurrent manner, or in one-after-another manner.

5.2 Preprocessing based indexing

A conspicuous characteristic of the above scheme is that we have to compute UR *on the fly*. In here, we present another indexing scheme, that is, we pre-compute the URs, and index them using R-tree. In here, we construct RA index at first, then we pre-compute UR and construct UR index. In the process of pre-computing URs, we can fully take advantage of the RA index. In this scheme, it is possible that a MO reports its' new location to server in the period of constructing UR index. For this issue, we differentiate two cases. (1) the UR of this MO has ever been pre-computed and indexed in UR index; (2) the UR of this MO has not been pre-computed. For this issue, it is easy to tackle. For instance, for the first case, we can re-compute this UR and update the current UR index right now, or we just store a label for it, we, based on label information, re-compute this UR and update UR index after we pre-computed and indexed all 'old' URs. Certainly, we also need update the location record in database. For the second case, we only need update the location record in database. Note that, in this scheme, i.e., preprocessing based indexing, we also construct two indices, i.e., RA index and UR index.

6 Performance study

In this section, we discuss the settings of our experiments and present the important performance results for PRQ over uncertain moving objects in constrained $2D$ space.

6.1 Experiment Settings

There are two types of datasets in our experiments, one is for representing RAs, another is for representing the locations of MOs. We use a number of polygons to denote the RAs, and let them uniformly distributed in the 10000×10000 2D space. Furthermore, we use a number of points to denote the locations of MOs, and let them randomly distributed in the 2D space but with an external constraint that these points cannot locate in any RA. For simulating the MOs with different characters, we randomly generate different distance thresholds for different MOs.

All codes used in our experiments are written in C++ language. All experiments are conducted on a laptop with 2.16GHz dual core CPU and 1.86GB of memory, running Windows XP. The page size is fixed to 4096 bytes. The maximum number of children nodes in R-tree is fixed to 50. Other parameters are illustrated in Table 1.

Table 2. Parameters Used in Our Experiments

Parameter	Description	Value
N	number of objects	$[1 \times 10^4, \dots, 5 \times 10^4]$
M	number of RA	$[1 \times 10^4, \dots, 5 \times 10^4]$
R_{size}	size of R	$[(100 \times 100), \dots, (500 \times 500)]$
RA_{edges}	edges of each RA	$[4, \dots, 64]$
N_{seed}	number of valid random points	$[10^2, \dots, 10^8]$
DT_j	distance threshold of O_j	$[20, \dots, 50]$

6.2 Results

We first present the experimental results when MOs are subjected to uniform distribution in Subsection 6.2.1, followed by presenting our experimental results when the pdf is Distorted Gaussian in Subsection 6.2.2. Note that, since the setting of this problem is in constrained 2D space, existing methods cannot support PRQ over uncertain moving objects in this setting, we will not compare our methods with existing methods.

6.2.1 Uniform Distribution

In terms of our methods, we compare the following several schemes: basic framework with quick method (BQ); basic framework with quick method and immediate indexing (BQII); basic framework with quick method and preprocessing based indexing (BQPI).

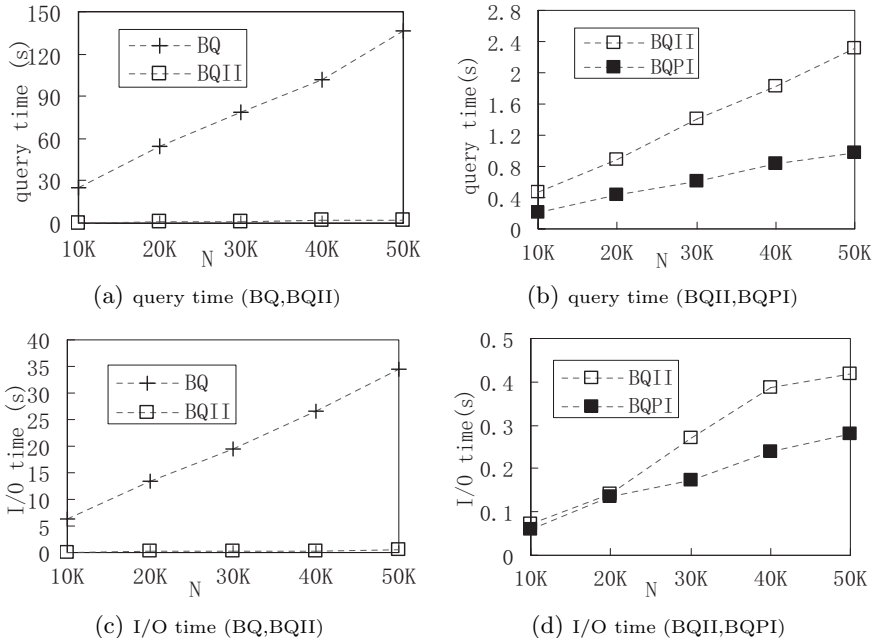


Fig. 10. Query and I/O performance vs. N

Impact of N For efficiently investigating the impact of N , we fix other parameters and only vary the value of N (from 10000 to 50000). Specifically, we let rectangle with 40×10 size as the RA, and set $M = 50000$. We generate randomly 50 rectangles with 500×500 size as the input of query, and we run 10 times for each test group, then compute the average query time and I/O time for estimating a single query. Figure 10 illustrates the results. Both query time and I/O time are increasing with the increase of N for the three schemes. The main reason is derived from the fact that more CMOs will locate in R when N increases and other conditions are constant. For these increased objects, we also have to fetch data from database (incurring more I/O time) and evaluate the probability (incurring more CPU time). BQII outperforms BQ (10(a) and 10(c)) since BQII utilize the R-tree, which contributes to the decrease of the number of fetching records from database (incurring less I/O time), and the decrease of comparing operations between the MBR of R and the MBRs of CMOs (incurring less CPU time). BQPI outperforms BQII (10(b) and 10(d)) since BQII evaluate UR *on the fly* (incurring more CPU time), which have to fetch RA data from database (incurring more I/O time). For the rest of experimental results, if BQPI outperforms BQII or BQII outperforms BQ, and if there is no other reason, we will not explain repeatedly the details for saving space.

Impact of M For well investigating the impact of M , we use similar test method as previous paragraph presented, but with a little modification. Specifically, we fix $N = 50000$ and vary the value of M (from 10000 to 50000). The results are

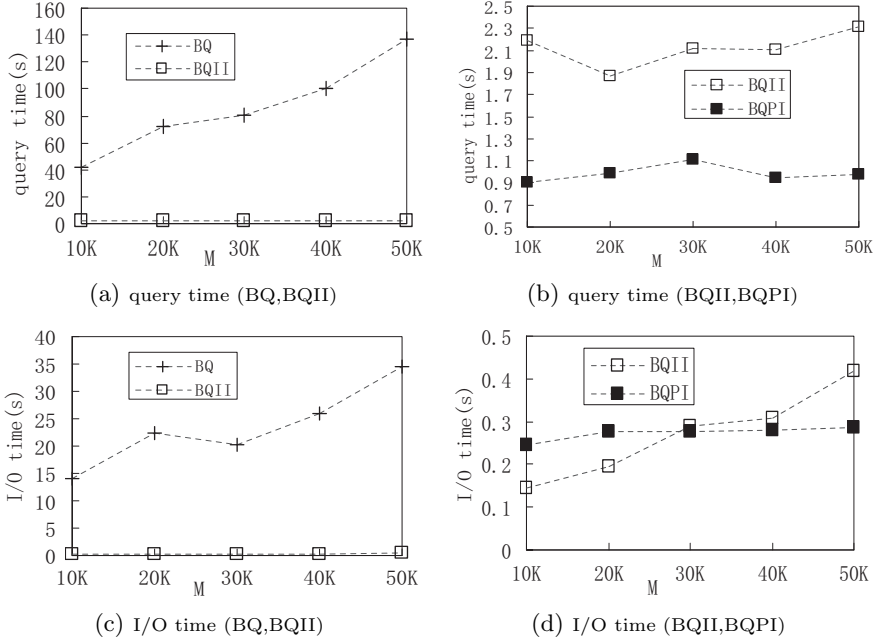


Fig. 11. Query and I/O performance vs. M

illustrated in Figure 11. The size of M has a great impact on BQ, but for BQII or BQPI, the query time is near to constant when we vary the size of M (11(a) and 11(b)). In particular, the I/O time for BQPI also is near to constant (11(d)), this is because BQPI index directly on MOs and URs, we need not fetch RA records from database. Note that, the I/O performance of BQPI does not always outperform that of BQII (11(d)). This is because, when M is a small value, the time of fetching UR record from database is larger than the sum of time fetching location records and fetching corresponding RA records. Though it is so, the query performance of BQPI is still outperforming that of BQII (11(b)). This is because BQPI need not compute the UR *on the fly*, which contributes to a big saving in CPU time, and this saving is large than the value that the I/O time of BQPI minuses that of BQII (when it is a positive number).

Impact of RA_{edges} We vary the number of edges (ranging from 4 to 64) in each RA for studying the impact of RA_{edges} . Specifically, We let $M = 50000$, and let equilateral polygon as RA. For each RA, it has the property that the distance from its' center to its' vertice is 20. For different test groups, we just vary the number of edges in each RA. Other parameters without stated in here is same with that in previous paragraph. Figure 12 illustrates the results. Both query time and I/O time are increasing as RA_{edges} increases for the three schemes. In terms of BQPI (12(b) and 12(d)), there are several reasons. First, RA itself will enlarge with the increase of the number of edges, since we set the distance from its' center to vertice is a fixed value, then, an equilateral polygon with

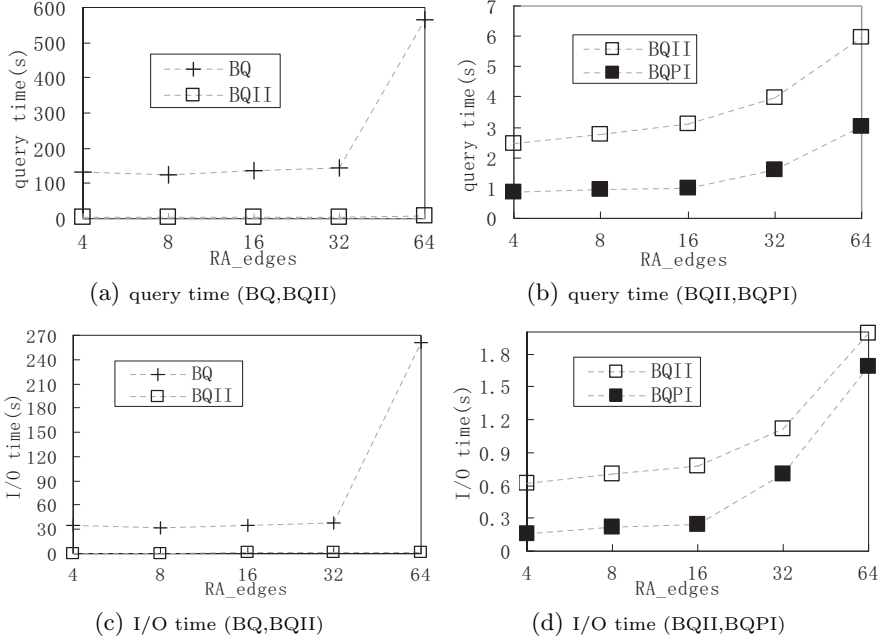


Fig. 12. Query and I/O performance vs. RA_{edges}

more edges will occupy more areas. Therefore, as the RA_{edges} increases, some RAs that do not intersect with EP_j , under the RA_{edges} with a small value, will possible intersect with EP_j , so we will have to evaluate the subtraction between EP_j and these RAs (incurring more CPU time). Second, with the increase of RA_{edges} , the complexity of UR should be upgraded, which results in taking more time to fetch UR record from database (incurring more I/O time).

Impact of R_{size} Figure 13 depicts the performance results when we vary the size of R . In here, we let rectangle with 40×10 size as the RA, and both M and N are set to 50000, we generate randomly 50 rectangles as the input of query. For different test groups, we vary the size of R , from “ 100×100 ” to “ 500×500 ”. Other parameters without stated in here are same with that in previous paragraph. We observe that, with the increase of R_{size} , both the query time and I/O time are increasing for the three schemes. This is because more CMOs will locate in R (with the increase of R_{size}), then more location records and corresponding RA records, or UR records, should be fetched from database (incurring more I/O time). In addition, for those increased CMOs, we also have to evaluate their probability (incurring more CPU time).

6.2.2 Distorted Gaussian Distribution

In the following experiment, we assume the *pdf* is *Distorted Gaussian* (*pdf*_{DG}(x, y) for short). The definition of *Distorted Gaussian* is derived from general Gaus-

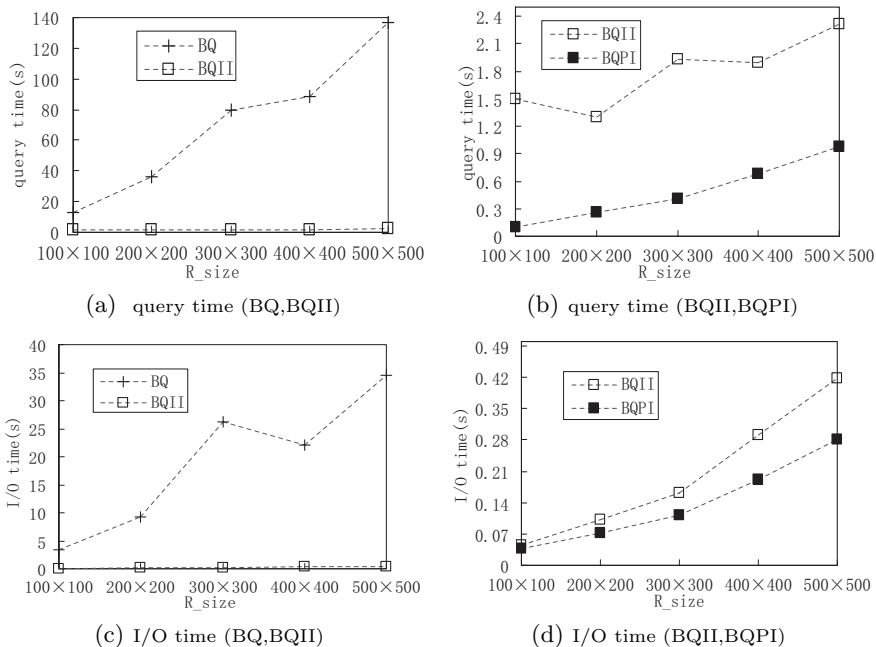


Fig. 13. Query and I/O performance vs. R_{size}

sian⁴. Given the *pdf* of general Gaussian is $pdf_G(x, y)$, and a coefficient λ , where $\lambda = \int_{\forall(x,y) \in UR_j} pdf_G(x, y) dx dy$, then we get the $pdf_{DG}(x, y)$ as follows.

$$pdf_{DG}(x, y) = \begin{cases} pdf_G(x, y) / \lambda, & \text{if } (x, y) \in UR_j \\ 0, & \text{otherwise} \end{cases} \quad (5)$$

In theory, we should have calculated the coefficient λ and translated $pdf_G(x, y)$ into $pdf_{DG}(x, y)$ for each MO. Fortunately, we neither need calculate it, nor need any translating for any MO in practice. The reason is that the λ will be eliminated when we substitute $pdf_{DG}(x, y)$ with $pdf_G(x, y) / \lambda$ in following formula.

$$p_j = \left(\sum_{i=1}^{N_2} pdf_{DG}(x_i, y_i) \right) \div \left(\sum_{i=1}^{N_1} pdf_{DG}(x_i, y_i) \right) \quad (6)$$

where N_1, N_2 are the number of random points that locating in UR_j and the IS_j , respectively (recall Subsection 4.4.2). In our experiment, the standard deviation of $pdf_G(x, y)$ (used for defining the $pdf_{DG}(x, y)$) is set to $DT_j/5$, the mean u_x and u_y is set to $L_j^{last}.X$ and $L_j^{last}.Y$, respectively.

Workload Error We investigate the workload error in order to find out appropriate value for parameter N_{seed} . Then, we use the chosen value to verify the query efficiency under Distorted Gaussian. Two kinds of common workload

⁴ The *pdf* of general Gaussian is $\frac{1}{2\pi\delta^2} e^{-\frac{(x-u_x)+(y-u_y)}{2\delta^2}}$, general Gaussian has an infinite input space, which is symmetric. However, the input space of *Distorted Gaussian* used in our experiment is limited to UR_j and it may be not symmetric.

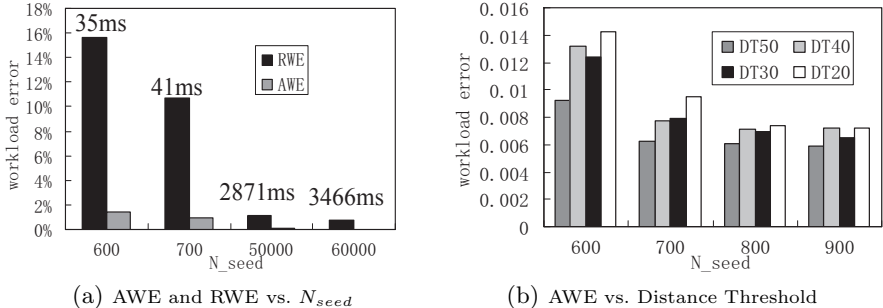


Fig. 14. Monte Carlo Method Workload Error Comparison

errors are relative workload error (RWE) and absolute workload error (AWE)⁵. We choose AWE to evaluate the efficiency of our proposed approaches. The main reason is derived from the fact that to ensure a very small RWE will take much more time than to ensure a same size AWE. In most cases, a small AWE is enough to satisfy our demand. We validate this by the following method.

We generate an object O_j with $DT_j = 20$ at the centre of $2D$ space and compute UR_j . Next, we generate a number 100 of query ranges which have same size (500×500 rectangle) and have different intersections with this UR_j . At first run, we get the real answer⁶ of each query by setting $N_{seed} = 10e + 8$. Next, we vary the size of N_{seed} to get several groups of AWEs and RWEs. When $N_{seed} = 700$, the AWE is 0.95% (i.e., 0.0095), and the RWE is 10.75% as shown in Figure 14(a). Obviously, it is unreasonable if we choose 10.75% as RWE. Otherwise, this means that returning a value of 89.25% will be tolerated even if the real value is 100%. Therefore, in order to get a smaller RWE, we have to increase N_{seed} . By doing so, we get RWE= 1.12% and RWE= 0.05% at $N_{seed} = 50000$. Therefore, for assuring a value 1% of RWE, we have to set $N_{seed} > 50000$ at least. However, even if we choose $N_{seed} = 50000$, and just for evaluating a single objects' probability, it takes about 2871 millisecond. In view of these, we choose AWE to estimate the returning results.

In addition, we vary the value of DT_j to verify the impact of DT_j on AWE (using similar method as above). Figure 14(b) shows that an object with smaller DT_j , as a whole, usually need larger N_{seed} if we want to assure same AWE. Based on this fact, we choose $N_{seed} = 700$ in our next experiment, which will ensure a number 0.01 of AWE.

Query Efficiency When pdf is *Distorted Gaussian*, we compare the following schemes: basic framework with Monte Carlo method and immediate indexing (BMII); basic framework with Monte Carlo method and preprocessing based indexing (BMPI). Since Monte Carlo method is only relevant to the evaluation of probability, the I/O efficiency is same with that under *uniform distribution*. So we just compare their query efficiency. In here, we present the performance re-

⁵ $RWE = \frac{|estimated\ value - real\ value|}{real\ value}$, $AWE = |estimated\ value - real\ value|$

⁶ In fact, this value is very closer to real value other than absolute real value.

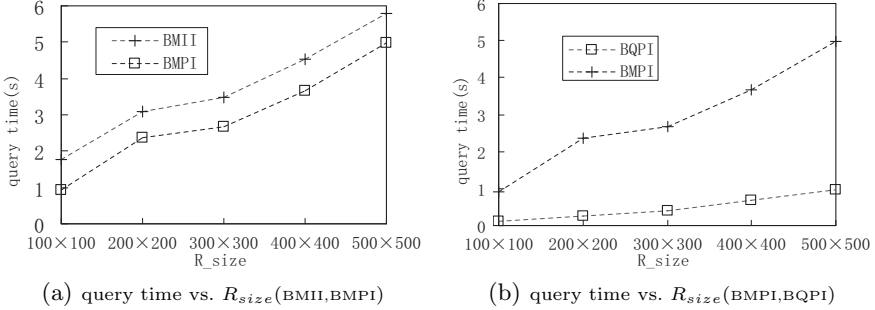


Fig. 15. Query Efficiency Comparison

sult when we vary the R_{size} . Other parameters (without stated in here) are same with those when we investigate the impact of R_{size} under *uniform distribution*. Figure 15(a) illustrates our result. As we expected, the query time are increasing with the increase of R_{size} for the two tactics, and BMPI outperforms BMII. The reason is similar to that discussed in Subsection 6.2.1. In addition, we compare the performance between BMPI and BQPI, all parameters are totally same except the *pdf*. Figure 15(b) depicts the result. We observe that the query time for the former is far more than that of later. This is because the time for evaluating a single object’s probability is relatively long when *pdf* is *Distorted Gaussian*.

7 Related Works

In terms of range query over uncertain moving objects, researchers have made considerable efforts [19, 20, 12, 21, 22, 16, 32, 23, 24, 13, 33–35, 18, 17, 25, 14, 36]. For example, Sistla et al. [20, 23] proposed MOST model for efficiently representing the location of moving objects, and they proposed a temporal query language, FTL, for providing more intuitive and simple query language, however, their approach just provides qualitative answer, i.e., certain object *may* or *must* locates in certain region at sometime rather than how much the probability is. Trajcevski et al. [24] proposed to model an uncertain trajectory as a 3D (2D for space, 1D for time) cylindrical body, their approaches also just give qualitative answer.

Wolfson et al. [14] presented a probabilistic method for processing range queries, they assumed all the objects were travelling on routes, their research belongs to “coarse-grained” query. Zheng et al. [25] represented the uncertainty of the objects moving along road networks as time-dependent probability distribution functions, and they proposed an indexing mechanism, UTH, for efficiently managing and retrieving massive trajectories, obviously, their research also belongs to “coarse-grained” query.

Pfoser et al. [12] proposed to represent the uncertain region of a moving object as a circle, and to represent the historical trajectories of moving objects as polylines, they focused on querying the past location of moving objects during

an interval of time. Recently, Zhang et al. [17] devised inference method for the prediction of future locations.

Cheng et al. [13] characterize the uncertainty of a moving object as a closed region with a probability function, and adopted VCI to manage the moving objects. Tao et al. [32] investigated probability threshold range query, they proposed probabilistic constrained rectangles (PCR), which contributes to pruning/validating a majority of nonqualifying/qualifying objects, and proposed an indexing technology, U-tree, for indexing uncertain objects and reducing I/O cost. Chen et al. [16] addressed location based range query, i.e., the location of querying issuer is not static. However, to the best of our knowledge, there is no prior work addressing PRQ over uncertain moving objects in constrained 2D space.

8 Conclusion

PRQ over uncertain moving objects is attracting extensive attentions, we, in this paper, make a more realistic assumption that objects are moving in constrained 2D space. We discuss technique for representing the different entities, and present a framework for query processing. We, by carefully analysing the geometry-topological relation between different entities, design elegant algorithms for computing the UR and IS. In order to obtain the probability, we discuss two methods, quick method and Monte Carlo method, which are used for different *pdf*. Moreover, we introduce two R-tree based indexing schemes for further improving the efficiency. We demonstrate through extensive experiments the correctness and effectiveness of our proposed approaches. In future, we will study other typical queries (such as KNN) over objects that are moving in constrained 2D space, these queries are more interesting and challenging.

References

1. Pitoura, E., Samaras, G.: Locating objects in mobile computing. *IEEE Transactions on Knowledge and Data Engineering (TKDE)* **13**(4) (2001) 571–592
2. Zhang, R., Jagadish, H.V., Dai, B.T., Ramamohanarao, K.: Optimized algorithms for predictive range and knn queries on moving objects. *Information Systems (Inf. Syst.)* **35**(8) (2010) 911–932
3. Gedik, B., Wu, K.L., Yu, P.S., Liu, L.: Processing moving queries over moving objects using motion-adaptive indexes. *IEEE Transactions on Knowledge and Data Engineering (TKDE)* **18**(5) (2006) 651–668
4. Wu, K.L., Chen, S.K., Yu, P.S.: Incremental processing of continual range queries over moving objects. *IEEE Transactions on Knowledge and Data Engineering (TKDE)* **18**(11) (2006) 1560–1575
5. Wang, H., Zimmermann, R.: Processing of continuous location-based range queries on moving objects in road networks. *IEEE Transactions on Knowledge and Data Engineering (TKDE)* **23**(7) (2011) 1065–1078
6. Tao, Y., Papadias, D., Sun, J.: The tpr*-tree: An optimized spatio-temporal access method for predictive queries. In: *International Conference on Very Large Databases (VLDB)*. (2003) 790–801

7. Mokhtar, H., Su, J., Ibarra, O.H.: On moving object queries. In: International Symposium on Principles of Database Systems (PODS). (2002) 188–198
8. Prabhakar, S., Xia, Y., Kalashnikov, D.V., Aref, W.G., Hambrusch, S.E.: Query indexing and velocity constrained indexing: Scalable techniques for continuous queries on moving objects. *IEEE Transaction on Computers (TC)* **51**(10) (2002) 1124–1140
9. Mokbel, M.F., Xiong, X., Aref, W.G.: Sina: Scalable incremental processing of continuous queries in spatio-temporal databases. In: ACM International Conference on Management of Data (SIGMOD). (2004) 623–634
10. Mokbel, M.F., Aref, W.G.: Sole: scalable on-line execution of continuous queries on spatio-temporal data streams. *The international Journal on Very Large Databases (VLDB J.)* **17**(5) (2008) 971–995
11. Hu, H., Xu, J., Lee, D.L.: A generic framework for monitoring continuous spatial queries over moving objects. In: ACM International Conference on Management of Data (SIGMOD). (2005) 479–490
12. Pfoser, D., Jensen, C.S.: Capturing the uncertainty of moving-object representations. In: International Symposium on Large Spatial Databases (SSD). (1999) 111–132
13. Cheng, R., Kalashnikov, D.V., Prabhakar, S.: Querying imprecise data in moving object environments. *IEEE Transactions on Knowledge and Data Engineering (TKDE)* **16**(9) (2004) 1112–1127
14. Wolfson, O., Sistla, A.P., Chamberlain, S., Yesha, Y.: Updating and querying databases that track mobile units. *Distributed and Parallel Databases (DPD)* **7**(3) (1999) 257–387
15. Zhang, Y., Lin, X., Tao, Y., Zhang, W.: Uncertain location based range aggregates in a multi-dimensional space. In: IEEE International Conference on Data Engineering (ICDE). (2009) 1247–1250
16. Chen, J., Cheng, R.: Efficient evaluation of imprecise location dependent queries. In: IEEE International Conference on Data Engineering (ICDE). (2007) 586–595
17. Zhang, M., Chen, S., Jensen, C.S., Ooi, B.C., Zhang, Z.: Effectively indexing uncertain moving objects for predictive queries. *The Proceedings of the Very Large Database Endowment (PVLDB)* **2**(1) (2009) 1198–1209
18. Abdessalem, Decreusefond, L., Moreira, J.: Evaluation of probabilistic queries in moving objects databases. In: International ACM Workshop on Data Engineering for Wireless and Mobile Access (MobiDE). (2006) 11–18
19. Chung, B.S.E., Lee, W.C., Chen, A.L.P.: Processing probabilistic spatio-temporal range queries over moving objects with uncertainty. In: International Conference on Extending Database Technology (EDBT). (2009) 60–71
20. Sistla, A.P., Wolfson, O., Chamberlain, S., Dao, S.: Modeling and querying moving objects. In: IEEE International Conference on Data Engineering (ICDE). (1997) 422–432
21. Trajcevski, G.: Probabilistic range queries in moving objects databases with uncertainty. In: International ACM Workshop on Data Engineering for Wireless and Mobile Access (MobiDE). (2003) 39–45
22. Chen, Y.F., Qin, X.L., Liu, L.: Uncertain distance-based range queries over uncertain moving objects. *Journal of Computer Science and Technology (JCST)* **25**(5) (2010) 982–998
23. Sistla, A.P., Wolfson, O., Chamberlain, S., Dao, S.: Querying the uncertain position of moving objects. In: Temporal Databases. (1997) 310–337

24. Trajcevski, G., Wolfson, O., Hinrichs, K., Chamberlain, S.: Managing uncertainty in moving objects databases. *ACM Transactions on Database Systems (TODS)* **29**(3) (2004) 463–507
25. Zheng, K., Trajcevski, G., Zhou, X., Scheuermann, P.: Probabilistic range queries for uncertain trajectories on road networks. In: *International Conference on Extending Database Technology (EDBT)*. (2011) 283–294
26. Margalit, A., Knott, G.D.: An algorithm for computing the union, intersection or difference of two polygons. *Computers and Graphics* **13**(2) (1989) 167–183
27. Vatti, B.R.: A generic solution to polygon clipping. *Communications of the ACM (CACM)* **35**(7) (1992) 56–6
28. Greiner, G., Hormann, K.: Efficient clipping of arbitrary polygons. *ACM Transactions on Graphics (TOG)* **17**(2) (1998) 71–83
29. Rappoport, A.: An efficient algorithm for line and polygon clipping. *The Visual Computer (VC)* **7**(1) (1991) 19–28
30. Liu, Y.K., Wang, X.Q., Bao, S.Z., Gombosi, M., Zalik, B.: An algorithm for polygon clipping, and for determining polygon intersections and unions. *Computers and Geosciences (GANDC)* **33**(5) (2007) 589–598
31. Hormann, K., Agathos, A.: The point in polygon problem for arbitrary polygons. *Computational Geometry* **20**(3) (2001) 131–144
32. Tao, Y., Xiao, X., Cheng, R.: Range search on multidimensional uncertain data. *ACM Transactions on Database Systems (TODS)* **32**(3) (2007) 15
33. Patroumpas, K., Sellis, T.K.: Prioritized evaluation of continuous moving queries over streaming locations. In: *International Conference on Scientific and Statistical Database Management (SSDBM)*. (2008) 240–257
34. Kalashnikov, D.V., Prabhakar, S., Hambrusch, S.E., Aref, W.G.: Efficient evaluation of continuous range queries on moving objects. In: *International Conference on Database and Expert Systems Applications (DEXA)*. (2002) 731–740
35. Wang, H., Zimmermann, R., Ku, W.S.: Distributed continuous range query processing on moving objects. In: *International Conference on Database and Expert Systems Applications (DEXA)*. (2006) 655–665
36. Trajcevski, G., Choudhary, A.N., Wolfson, O., Ye, L., Li, G.: Uncertain range queries for necklaces. In: *International Conference on Mobile Data Management (MDM)*. (2010) 199–208